SCK • CEN
STUDIECENTRUM VOOR KERNENERGIE
CENTRE D'ÉTUDE DE L'ÉNERGIE NUCLÉAIRE

ON THE USE OF THE MASTER CURVE BASED ON THE PRECRACKED CHARPY SPECIMEN

R. Chaouadi, M. Scibetta and E. van Walle
SCK•CEN
Boeretang 200
2400 Mol, Belgium

R. Gérard
Tractebel Energy Engineering
Avenue Ariane 7
1200 Bruxelles, Belgium

Presented at the 1999 ASME Pressure Vessel and Piping Symposium
August 1-5, 1999, Boston, Massachusetts, USA.

BLG-820

ON THE USE OF THE MASTER CURVE BASED ON THE PRECRACKED CHARPY SPECIMEN

R. Chaouadi, M. Scibetta and E. van Walle
SCK•CEN
Boeretang 200
2400 Mol, Belgium

R. Gérard
Tractebel Energy Engineering
Avenue Ariane 7
1200 Bruxelles, Belgium

Presented at the 1999 ASME Pressure Vessel and Piping Symposium
August 1-5, 1999, Boston, Massachusetts, USA.

BLG-820

PVP-Vol. 393, Fracture, Fatigue and Weld Residual Stress
ASME 1999, pp. 35-46

ON THE USE OF THE MASTER CURVE BASED ON THE PRECRACKED CHARPY SPECIMEN

Rachid Chaouadi, Marc Scibetta, and Eric van Walle
SCK•CEN
Boeretang 200
2400 Mol, Belgium

Robert Gérard
Tractebel Energy Engineering
Avenue Ariane, 7
1200 Bruxelles, Belgium

ABSTRACT

Recently, a large worldwide has focused on evaluation of the use of the Master Curve approach to characterize fracture toughness of ferritic steels in the transition regime. This was acknowledged by the recent release of the ASTM Standard Test Method for Determination of Reference Temperature, T_0, for Ferritic Steels in the Transition Range (E1921). The present work aims to investigate the use of the Charpy specimen along with the Master Curve approach to derive the fracture toughness behavior of reactor pressure vessel steels. Therefore, four well characterized and documented reactor pressure vessel steels were selected. A large experimental program to measure fracture toughness with Charpy size specimens was carried out. Four important aspects were investigated:

- the T_0 determination as a function of test temperature;
- the E1921 specimen size requirement (factor M=30);
- the censoring procedure for specimens not satisfying the E1921 size requirements;
- the estimation of the fracture toughness lower bound, and its comparison to the ASME K_{IC} curve.

It is found that within the experimental and statistical uncertainties, the reference temperature T_0 is not affected by the test temperature, even when data are not valid according to E1921 requirements. By application of the censoring procedure, the determination of the reference temperature may lead to non conservative results. Comparison to larger specimen size suggests the use of M=60 rather than 30 to limit the loss of constraint, in agreement with finite element calculations. Nevertheless, the differences are not large enough to be statistically significant. The lower bound based on the Master Curve is very close to the experimental lower bound, while the ASME K_{IC} curve tends to be over conservative. Replacing RT_{NDT} by the new index, RT_{To}, in the ASME K_{IC} equation reduces this over conservatism.

INTRODUCTION

Characterization of fracture toughness in the transition regime suffers from the size dependence of the results. Indeed, the fracture toughness behavior is affected by two important inter-related phenomena: the statistical size effect and loss of constraint.

SCK•CEN has put an extensive effort in characterizing fracture toughness behavior using Charpy size specimens. The choice of the Charpy geometry to measure fracture toughness is motivated by the following two important points:

- The Charpy specimen is used for monitoring reactor pressure vessel degradation induced by neutron irradiation;
- Reconstitution technology allows re-fabrication of new samples from broken Charpy halves, increasing the number of specimens.

Therefore, various well documented and characterized reactor pressure vessel steels were selected in order to demonstrate the reliability of the methodology. The main geometry is the PreCracked Charpy v-notch (PCCv) specimen (10×10×55 mm). In addition, the 3 Point Bend (3PB) specimen (W=20 mm, B=15 mm, 20% side grooved) and the Compact Tension (CT) specimen were tested for comparison.

The main objective of this work is to investigate the use of the Master Curve, developed by Wallin [1], for fracture toughness characterization of the transition regime. In particular,

- how does the reference temperature, T_0, vary with test temperature?
- is the loss of constraint well evaluated through the factor M=30?
- does the censoring procedure for specimens not satisfying the E1921 [2] size requirements lead to consistent results?
- how does the ASME K_{IC} lower bound curve compare to experimental data and to predicted curves?

Table 1. Chemical composition.

material	C	Si	P	S	Cr	Mn	Ni	Cu	Mo
22NiMoCr37	0.22	0.23	0.006	0.004	0.39	0.88	0.84	0.08	0.51
JRQ	0.18	0.24	0.017	0.004	0.14	1.42	0.84	0.14	0.51
A533B (JSPS)	0.24	0.41	0.028	0.023	0.08	1.52	0.43	0.19	0.49
73W	0.10	0.45	0.005	0.005	0.25	1.56	0.60	0.31	0.58

Table 2. Mechanical properties at ambient temperature.

material	orientation	yield stress σ_y (MPa)	tensile strength σ_u (MPa)	elongation ε_t (%)	reduction of area RA (%)
22NiMoCr37	L	455	609	20	73
JRQ	T	484	625	19	73
A533B (JSPS)	T	460	640	18	58
73W	T; L; S	490	600	22	68

MATERIALS

Four well documented and characterized reactor pressure vessel steels were selected:

- 22NiMoCr37: This material was extensively investigated, in particular through two round robin exercises related to the local approach to fracture, and to fracture toughness in the ductile to brittle transition regime [3].
- A533B Cl.1(JSPS): This steel was used in the Japanese round robin organized by the Japan Society for the Promotion of Science [4]. It has a low upper shelf energy (70J) as a result of high S and P concentrations.
- A533B Cl.1(referred as JRQ): This IAEA monitor material is well known within the IAEA community. It was also used in a round robin related to fracture toughness [5].
- 73W Weld: This weld was extensively characterized by ORNL [6], in the un-irradiated as well as the irradiated condition.

The chemical composition and the mechanical properties are reproduced in Table 1 and 2, respectively.

For each steel, at least ten tensile specimens were tested over the temperature range [–200 to +300 °C]. The variation of yield stress, σ_y, with test temperature is fitted with the following equation:

$$\sigma_y = A + B \exp\left[C\,T\right]$$

where σ_y, is expressed in MPa and the temperature T in °C. The constants A, B and C for each material are given in Table 3. These equations will be used later to determine the maximum K_J capacity of the various specimens. The strain hardening exponent, n, is obtained from the yield to ultimate stress ratio, using the following expression [7]:

$$\frac{\sigma_y}{\sigma_u} = \exp\,(n)\left[\frac{0.002 + \frac{\sigma_y}{E}}{n}\right]^n$$

Table 3. Fitting constants for the evolution of yield stress with temperature.

material	N	A	B	C
22NiMoCr37	10	409.37	55.50	–0.0118
JRQ	12	443.55	39.26	–0.0127
A533B (JSPS)	17	423.57	40.82	–0.0125
73W	19	466.62	35.73	–0.0129

Notes: N is the number of specimens tested over the temperature range [–200 to +300 °C].

The material is assumed to follow a power law type behavior. The variation of strain hardening exponent with test temperature is fitted with the following polynomial equation:

$$n = A_0 + A_1\,T + A_2\,T^2 + A_3\,T^3 + A_4\,T^4 + A_5\,T^5$$

where the constants A_i are given in Table 4. Figure 1 shows the evolution of the yield stress and the strain hardening exponent as a function of temperature.

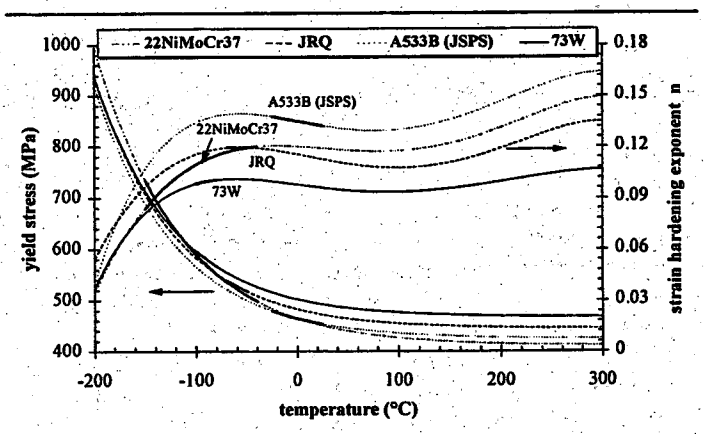

Figure 1. Yield stress and strain hardening coefficient as a function of temperature. Temperature range for K_{Jc} tests **in bold.**

Table 4. Fitting constants for the strain hardening exponent.

material	A_0	A_1 ($\times 10^{-4}$)	A_2 ($\times 10^{-7}$)	A_3 ($\times 10^{-9}$)	A_4 ($\times 10^{-11}$)	A_5 ($\times 10^{-14}$)
22NiMoCr37	0.120	−0.340	−5.683	7.524	−0.903	−1.623
JRQ	0.116	−1.132	−3.012	7.460	−1.069	−1.419
A533B (JSPS)	0.135	−1.145	−0.477	9.151	−2.510	0.981
73W	0.098	−0.783	−0.257	5.249	−1.797	1.583

Table 5. Impact properties.

material	orientation	N(1)	USE (J)	T_{68J} (°C)	T_{41J} (°C)	T_{28J} (°C)	$T_{50\%}$ (°C)	$T_{0.89mm}$ (°C)	RT_{NDT} (°C)
22NiMoCr37	L-S	12	194	−38	−50	−58	−20	−43	−40 [8]
JRQ	T-L	12	215	−4	−19	−30	20	−11	−15 [9]
A533B (JSPS)	T-L	19	72	101	34	16	43	46	68(2)
73W	T-L	12	142	−18	−34	−43	−12	−28	−34 [6]

Notes: (1) N is the number of tested specimens.
(2) RT_{NDT} is estimated from the Charpy impact data: $RT_{NDT} = \max(T_{68J}; T_{0.89mm}) - 33°C$ [10]. Pellini drop weight tests were not performed for A533B (JSPS).

The impact properties derived from Charpy tests are given in Table 5. The transition behavior of the impact energy is shown in Figure 2. This Figure clearly illustrates the differences between the four steels, in particular the upper shelf energy level and the various transition temperatures. In the last column, the Reference Temperature of Nil-Ductility Transition, is also given. The latter is controlled by the Pellini drop weight test except for A533B (JSPS) for which only Charpy impact data were available.

experimental

Most of the fracture toughness tests are performed on precracked Charpy specimens loaded in three point bending. The tests are carried out in an Instron tensile machine under controlled displacement at a constant crosshead speed of 0.2 mm/min. The specimens are precracked by fatigue up to a "crack length-to-width" ratio close to 0.5. For most specimens, the stress intensity factor during fatigue is maintained below 25 MPa$\sqrt{m}$. During the last 0.6 mm of precracking, the stress intensity factor is kept below 18 MPa$\sqrt{m}$. A few samples were precracked above these values but fracture occurs well above the $K_{fatigue}$. Except for the 22NiMoCr37 samples, all specimens are 20% side grooved prior to testing. The specimen is maintained at the test temperature for at least 30 minutes prior to loading. During this period and during testing, the temperature remains well within ±1°C of the nominal value. The specimen is immediately unloaded after unstable crack initiation corresponding to cleavage fracture. The specimens were heat tinted at 290°C for 20 minutes and broken at liquid nitrogen temperature. The initial crack length and the eventual ductile crack extension prior to cleavage are measured on the broken surface using the 9-point method.

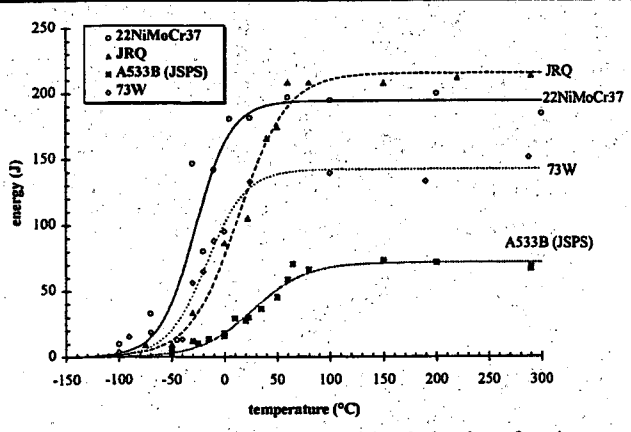

Figure 2. Charpy impact energy transition behavior of various reactor pressure vessel steels. Note that the A533B (JSPS) material exhibits a low upper shelf energy and a high transition temperature.

The J-integral is calculated from:

$$J = \frac{K^2(1-\nu^2)}{E} + \frac{\eta U_{pl}}{B_n(W-a_0)}$$

where $\eta = 2$ † for SENB geometry and $\eta = 2 + 0.522(1 - a_0/W)$ for the CT specimen. a_0 is the initial crack length, B_n and W are respectively the specimen net thickness and width. U_{pl} is derived from area under the load versus load line displacement curve from which the elastic part is subtracted. For the SENB geometry, the load line displacement (LLD) is derived from the crack mouth opening displacement (CMOD) using the following relation:

$$LLD = \frac{CMOD \quad S/4}{r_p(W-a_0) + a_0 \cos\left[\text{a tan}\left(\frac{CMOD/2}{r_p(W-a_0)+a_0}\right)\right]}$$

which can be approximated by:

† The E1921 recommends use of $\eta = 1.9$. However, as will be indicated later, a better agreement is found with $\eta = 2$ when LLD is derived from CMOD.

$$LLD \approx \frac{CMOD \quad S/4}{r_p(W - a_0) + a_0}$$

where S is the span and the rotational factor r_p=0.44.

An equivalent elastic plastic stress intensity factor K_{Jc} is then derived from the J-integral using:

$$K_{Jc} = \sqrt{\frac{JE}{1-\nu^2}}$$

where ν is the Poisson ratio (ν=0.3) and E is the elastic modulus (E=210 GPa for 22NiMoCr37 and JRQ, E=206 GPa for A533B (JSPS) and E=207–0.06 T(°C) for 73W [6]). Here, the plane strain rather than plane stress elastic modulus is used. This is more appropriate as plane strain conditions are prevailing at the crack tip. For consistency, all the data reported here are evaluated using this relation (PCCv as well as CT).

3D finite element calculations performed by Nevalainen and Dodds [11] and Koppenhoefer and Dodds [12] suggest the following η values for the deep cracked SENB geometry: η=1.9 for plain sided, and η=2 for side grooved samples. By using the above relations for J, LLD and K_{Jc}, and taking η=2, finite element calculations have shown a very good agreement with K based on the J contour integral. In the range of interest, the fracture toughness is underestimated by less than 2% (conservative side).

Two validity conditions are given in the ASTM E1921 standard [2] in relation to the specimen size:

- the maximum K_J level relative to the specimen size:

$$K_{J\,limit} = \sqrt{\frac{\sigma_y E (W - a_0)}{M}}$$

where, according to E1921, M=30.

- the maximum ductile crack extension:

$$\Delta a_{max}^{ductile} = 0.05 (W - a_0)$$

Specimens that do not satisfy these requirements can still be used in a censoring procedure. This is done by replacing the K_{Jc} values by the $K_{J\,limit}$ and calculating K_0 using:

$$K_0 = \left[\sum_{i=1}^{N} \frac{(K_{Jc(i)} - 20)^4}{r - (1 - \ln(2))} \right]^{1/4} + 20$$

where N is the total number of tests and r the number of 'valid' data.

Due to the limited number of specimens usually tested, a confidence interval should be associated with T_0. In the ASTM E1921 standard, the standard deviation for estimates of T_0 is approximated by $\beta/\sqrt{N}$. For a 95% confidence level, the ΔT_0 temperature deviation is:

$$\Delta T_0 = \frac{\beta}{\sqrt{N}} \alpha = \frac{1.6449 \times \beta}{\sqrt{N}}$$

where β varies between 18 and 22 depending on K_{Jmed} [2]. This relation was verified using experimental data and a Monte Carlo simulation [3].

One of the main advantages of using the Master Curve is that it provides confidence bounds. This is extremely important when safety assessment issues are addressed. For a specific level of probability, the fracture toughness curve is given by:

$$K_{X\%} = C_1 + C_2 \exp\left[0.019 (T - T_0)\right].$$

where C_1 and C_2 are constants: C_1=23.5 and C_2=24.5 for X=1% and C_1=25.4 and C_2=37.8 for X=5%

The best known lower bound curve is probably the K_{IC} ASME curve which is indexed by the RT_{NDT}. This curve is given by [9]:

$$K_{IC} = 36.48 + 22.78 \exp\left[0.036 (T - RT_{NDT})\right].$$

However, this curve is found too conservative in many cases. Recently, Kirk et al. [13] have assembled a large database of RPV fracture toughness data suggesting that the replacement of RT_{NDT} by a T_0-based index, RT_{To} (RT_{To}=T_0+19.4°C) in the ASME lower bound curve leads to a better agreement with experimental results.

RESULTS

All specimens were analyzed following a similar procedure. Most of the ASTM E1921 testing recommendations were fulfilled as well as the evaluation procedure, in particular for determining the reference temperature T_0. The reference toughness values (K_0) that are given in this paper refer to 1T adjusted values. Additionally, the shape parameter, or Weibull modulus for measuring the scatter is also determined using the maximum likelihood method. However, m was taken equal to 4 for the determination of T_0 and K_0.

The Master Curve approach is then applied to determine the reference temperature following the ASTM E1921 standard procedure. The fracture toughness test data are first normalized to one reference size, namely 1T (25 mm). The use of a small specimen generally results in significant loss of constraint. Data that are outside the validity range can still be used by applying an adequate censoring procedure. Here, four different censoring procedures are used for T_0 determination:

Method 1. all data are taken into account: no censoring is applied;
Method 2. the censoring procedure is applied following the E1921 recommendations: N is the total number of tests, r is the number of valid tests;
Method 3. the censoring procedure is similar to E1921 one except that r is substituted by N;
Method 4. the censoring procedure is similar to E1921 one except that N is substituted by r: only 'valid' data are considered.

For each material, three aspects of the Master Curve approach will be investigated. First, the comparison of the fracture toughness data to the Master Curve and associated probability bounds. Second, as at least two test temperatures were selected, how test temperature affects the reference temperature determination. Finally, the ASME K_{IC} lower bound curve based on the RT_{NDT} is compared to the 5% and 1% probability curves, and to the new proposal for replacing RT_{NDT} by RT_{To} [13].

22NiMoCr37 material

This testing program (see Table 6) was selected for comparison with the European round robin data [14]. Specimens are taken in the L-S orientation in the 1/4 to 3/4 thickness of the plate. All PCCv specimens are plain sided except 6 samples tested at −110°C (20% side grooving). Additionally, two series of nine 0.5T-CT plane sided specimens are tested for comparison.

Table 6. Test matrix: 22NiMoCr37.

test temperature	PCCv	CT
−150	8	
−125	7	
−110	12	
−90	8	9
−60	9	9
−40	8	

All specimens are plain side except 6 PCCv tested at 110°C that were 20% side grooved.

Most of the 22NiMoCr37 specimens do not satisfy the crack front straightness requirement of E1921. This is mainly due to the small size of the specimens and the absence of side grooving. According to E1921, the data that do not satisfy the crack front straightness should be discarded. The requirement is found to be too severe. Indeed, as will be shown later, this does not seem to significantly effect the results.

The observation of the fracture surfaces of small samples in order to determine whether single or multiple initiation occurred is more difficult than with large samples. At −150°C, the fracture surface is flat and no single initiation site could be localized. Between −125 and −91°C, the fracture surface becomes more irregular, but a single initiation site is still difficult to identify. Above −60°C, a single crack initiation site is found.

The results in terms of fracture toughness versus temperature are shown in Figure 3. All data are adjusted to 1 inch (25 mm) thickness. The 1T-adjusted $K_{J\ limit}$ for each geometry is also shown. All specimens failed by cleavage except two specimens tested at −40°C which were interrupted after significant ductile crack extension. A large number of specimens failed above the limit K_J-level according to E1921, necessitating data censoring.

In the test temperature range where loss of constraint is limited, the number of specimens is chosen to comply with the E1921 requirement. Therefore, 8 samples are tested at −150°C while at −125°C, 7 samples are tested. If crack front uniformity is not taken into consideration, all these data can be considered as valid according

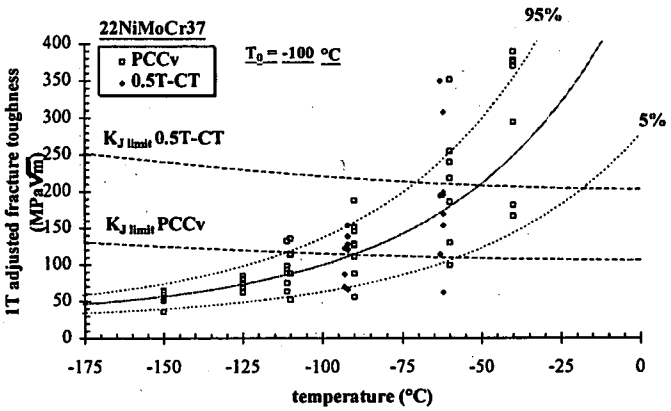

Figure 3. Fracture toughness behavior of 22NiMoCr37 in the transition regime is well described by the Master Curve and associated probability bounds.

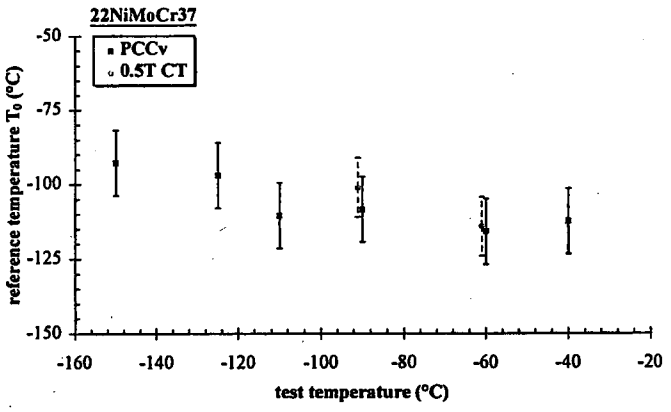

Figure 4. Effect of test temperature on the reference temperature T_0. No significant effect is found.

to E1921 requirements. At −110°C, twelve PCCv samples are tested among which 6 were 20% side grooved. Here, two samples do not satisfy the size requirement. When no censoring is applied, T_0=−110 °C. By censoring according to E1921, T_0 does not change. If r is considered instead of N in the K_0 relation, T_0=−107. Finally, if only the 10 'valid' data points are considered, T_0=−103°C. At higher test temperatures, the number of 'valid' data decreases such that the E1921 requirement on the minimum number of 'valid' data point is not fulfilled anymore. Consequently, the censoring procedure cannot be applied. Nevertheless, T_0 does not vary much in comparison to that determined at lower test temperatures. Figure 4 shows the results of Table 7 including their confidence interval, ΔT_0. It is important to emphasize that the differences observed here are not statistically significant. Globally, the reference temperature T_0 is within the expected confidence limit. The reference temperature based on these data can be estimated as T_0=−100°C (based on specimens tested at −150, −125°C and −110°C). Table 7 summarizes the results of this evaluation of the reference temperature using various data sets. The K_0 and Weibull slope (scatter parameter), m, is also given. For each data set, the number of data satisfying the E1921 size requirements is indicated together with the censoring procedure that is applied.

Table 7. Parameters characterizing fracture toughness of 22NiMoCr37 in the transition regime.

specimen	N	T	T_0	K_0	m	method	remark
	8	−150	−92.7	56.8	5.1	1	non uniform crack front
	7	−125	−97.0	76.0	7.5	1	non uniform crack front
	12	−110	−110.4	108.3	3.6	1	10 PCCv satisfy $K_{J\ limit}$
	12	−110	−107.4	104.0	4.1	3	censoring: r=N=12
PCCv	12	−110	−110.3	108.1	4.1	2	censoring E1921: N=12, r=10
	10	−110	−103.2	98.4	4.1	4	censoring: N=r=10
	8	−90	−109.6	142.2	3.1	1	3 PCCv satisfy $K_{J\ limit}$
	9	−60	−115.8	252.6	3.2	1	1 PCCv satisfies $K_{J\ limit}$
	8	−40	−114.7	348.4	4.5	1	all not valid (2 ductile)
	6	−40	−112.4	334.5	3.7	1	2 ductile discarded
	9	−91	−101.1	123.9	3.8	1	all valid per E1921
	9	−60	−114.2	245.7	2.2	1	7 CT satisfy $K_{J\ limit}$
CT	7	−60	−93.0	174.6	3.5	4	censoring: N=r=7
	9	−60	−96.4	184.3	4.0	3	censoring: r=N=12
	9	−60	−100.1	195.4	4.0	2	censoring E1921: N=9, r=7

Notes: N is the number of specimens, T is the test temperature, T_0 is the reference temperature, K_0 the normalization fracture toughness and m the Weibull modulus.

Comparison with 0.5T CT specimens tested by [15] at −91 and -60°C show that the results closely agree with those of the PCCv samples (see Table 7 and Figure 4). CT samples result in T_0=−101°C. Note that at −60°C, one CT specimen exhibited a very low K_J-value. Unfortunately, the number of available specimens is too limited to perform 12 additional tests as requested by E1921.

As already mentioned, the PCCv specimens are not side grooved. This was deliberately chosen in order to be compared with the test results generated within the European round robin on the same material [3]. As a consequence, most of PCCv samples exhibit a non uniform crack front. According to E1921, these data should be discarded. However, Table 7 shows that they are in very good agreement with CT specimens.

In Figure 5, the measured fracture toughness data are plotted as a function of test temperature. These data are compared to the 5% and 1% curves based on T_0=−100°C and the K_{IC} ASME curves indexed by RT_{NDT} and RT_{To}. If the CT sample that exhibited a very low toughness is ignored, the agreement between experimental data and these lower bound curves is very good. However, the RT_{NDT} based ASME curve is very conservative in comparison to the other curves. Note the excellent agreement between the 1% curve and the RT_{To} based K_{IC} ASME curve in the [−150 to −75 °C] test temperature range.

JRQ material

This plate material, fabricated in Japan, is the monitor material chosen by the IAEA, in particular within the CRP-III and IV research programs [5,16]. To reduce the material variability, all specimens were taken from the 1/4 and 3/4 thickness. Three geometries are tested beside tensile and impact Charpy samples: PCCv, 3PB, and CT. The specimens are taken in the T-L orientation in the 1/4 to 3/4 thickness of the plate. All specimens are 20% side grooved. Two test temperatures are selected: −70 and −50°C. At least 6 samples were tested per temperature. The test matrix is given in Table 8.

Table 8. Test matrix: JRQ.

test temperature	PCCv	3PB	1/2T-CT
−70	6	6	9
−50	6	6	11

Notes: All specimens are 20% side grooved.
PCCv and CT are taken from the CRP-IV block.
3PB are taken from the ESIS block.

Determination of the Master Curve parameters is performed according to E1921. The results are summarized in Table 9. For the PCCv, the reference temperature, calculated using PCCv tested at −70°C, is T_0=−54°C. For the CT samples, all data satisfy the E1921 requirements. However, at −70°C, one sample exhibited a very high

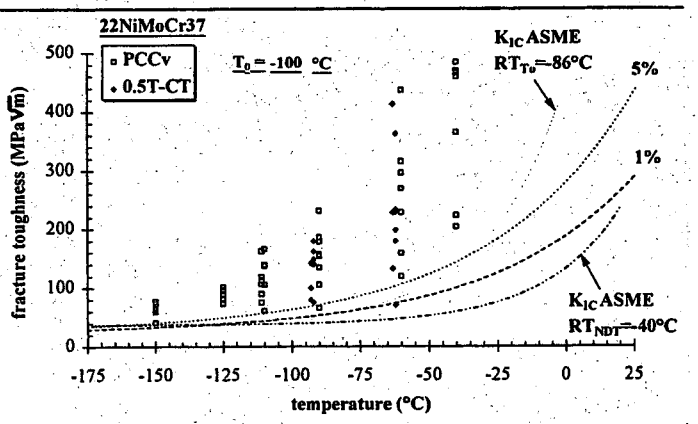

Figure 5. Comparison of fracture toughness data to lower bound curves: ASME K_{IC} versus probability curve.

Table 9. Master curve transition parameters for JRQ material.

geometry	N	T	T_0	K_0	m	method	remark
PCCv	6	−70	−53.8	87.4	2.4	1	valid per E1921
	6	−50	−63.2	129.5	5.7	1	2 PCCv satisfy $K_{J\ limit}$
CT	11	−70	−54.6	88.2	2.9	1	valid per E1921
	10	−70	−41.9	76.0	4.6	1	valid per E1921, outlier discarded
	9	−50	−43.7	99.0	3.5	1	valid per E1921
3PB	6	−70	−50.7	84.2	7.0	1	valid per E1921
	6	−50	−64.1	131.2	3.2	1	valid per E1921

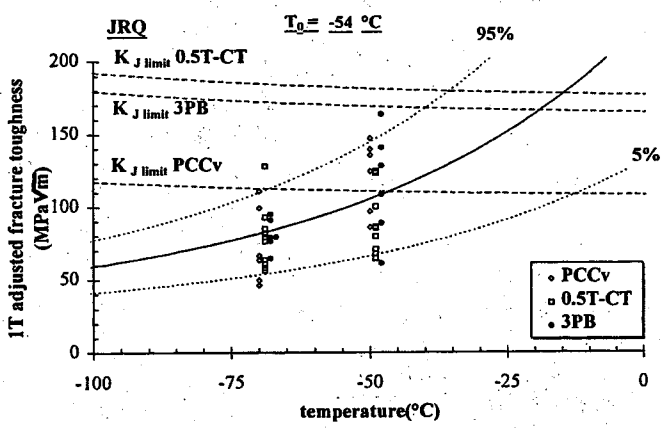

Figure 6. Master curve and associated confidence bounds for JRQ plate material.

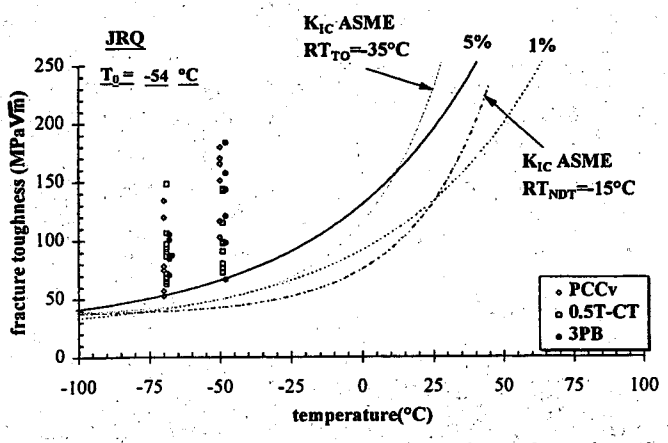

Figure 7. Comparison of fracture toughness data to lower bound curves: ASME K_{IC} versus probability curve.

K_{Jc} value. This data point significantly affects the value of T_0. While T_0=−43°C for specimens tested at −50°C, it varies from T_0=−55 to −42°C depending of whether this data point is taken into consideration or discarded. This data point can be considered an outlier. Indeed, by calculating individual T_0 for each sample, this 'outlier' point lies outside the 2σ confidence interval on average T_0.

Examination of 3PB data show a very good agreement with PCCv data. However, JRQ material is known to be quite inhomogeneous. It should be mentioned that PCCv and CT specimens are taken from the same block (CRP-IV block) while the 3PB specimens are manufactured from another one (ESIS block). Therefore, material inhomogeneity and geometry effects are difficult to separate.

Given the limited number of specimens, it is difficult to attribute the 15°C difference between T_0 determined using PCCv and T_0 from CT samples to the specimen size or to the material inhomogeneity. It will be shown later that the difference most probably results from the specimen size rather than material variability.

In Figure 6, the Master Curve and associated 95 and 5% bounds compared to the 1T adjusted experimental data show a good agreement (T_0 is taken as −54°C).

As for 22NiMoCr37, the lower bound curves are consistent with the experimental data, and the RT_{NDT} based K_{IC} ASME curve is very conservative (see Figure 7). Here also, up to −25°C, the 1% curve and the RT_{To}-based curve are identical.

Table 10. Test matrix: A533B (JSPS).

	SCK•CEN	JSPS Round Robin [4]			
test temperature	PCCv	0.5T CT	1T CT	2T CT	4T CT
−120	6	--	--	--	--
−25	10	18	16	2	--
0	20	23	24	6	2
+25	10	12	12	2	1

Number of specimens tested within the JSPS round robin are also indicated. All PCCv samples are 20% side grooved except at 0°C where 10 samples were plain sided.

A533B (JSPS) material

This material, used by the Japan Society for the Promotion of Science [4], is characterized by a high transition temperature and a low upper shelf. This is very interesting as irradiation induces such degradation in RPV steels. Forty PCCv samples of similar orientation (T-L) were manufactured from the broken CT samples and tested in the temperature range of interest [17]. In addition, six samples were tested at −120°C where fracture occurs in the linear elastic regime. All specimens were 20% side grooved except 10 samples tested at 0°C. The test matrix is given in Table 10.

At −120°C and −25°C, all samples fail in a brittle mode, without any ductile extension prior cleavage. At 0°C and +25°C, many samples exhibit a pop-in behavior. At +25°C, most samples exhibit ductile crack growth prior to cleavage. The data analysis in terms of T_0, K_0 and m for each geometry, size and test temperature are

gathered in Table 11. Figure 8 shows the 1T-adjusted fracture toughness data as a function of test temperature.

At −120°C, the $K_{J\ med}$ is very low and, consequently, no size correction is applied, as recommended by E1921. According to E1921, these data should not be used, as the uncertainty on T_0 is very high. At −25°C, all samples fail below the $K_{J\ limit}$ except one which is slightly above. The censoring procedures show that E1921 leads to non conservative values in comparison with not censoring the data. At 0°C, among the 20 PCCv specimens, only 7 samples lie below $K_{J\ limit}$. Here, the censoring procedure according to E1921 has no effect on T_0. At +25°C, all PCCv are not valid. On the other hand, most of the CT samples tested within the JSPS round robin comply with the E1921 requirements. The T_0 values determined with various data sets vary within 2 to 14°C, The mean value being T_0=8°C. The PCCv specimens result in T_0=−7°C, in compliance with E1921. Figure 8 shows how the Master Curve and its 95% confidence bounds compare to the experimental data. As with JRQ, a shift of 15°C between the two geometries is observed. Figure 9 shows the effect of test temperature and specimen geometry and size on the T_0 determination.

Figure 10 compares the fracture toughness data to the predictive lower bound curves. The experimental data are well bounded with the various curves, with the K_{IC} ASME curve based on RT_{NDT} being the most conservative.

73W weld material

The 73W weld material is one of the two high-Copper submerged-arc welds thoroughly investigated at ORNL within the 5th irradiation series of HSSI program [6]. Some of the broken samples, un-irradiated as well as irradiated large CT specimens, and a small block for Charpy size manufacturing was provided by ORNL. Reconstitution technology allowed us to machine Charpy specimens from the broken CT specimens. All specimens are taken in the T-L orientation. Details on fabrication and test results can be found in [18, 19]. The PCCv test results analyzed here were not reconstituted. Table 12 summarizes the data analysis. Eight PCCv specimens tested at −100°C lead to T_0=−69°C. At −80°C, of 11 PCCv samples tested, 4 fail above the $K_{J\ limit}$ level. If all data are considered regardless their validity (in terms of $K_{J\ limit}$), T_0 is found equal to −89°C. This results in a 20°C shift in comparison with −100°C data. The application of the censoring procedure according to E1921 slightly affects T_0. The best agreement with −100°C data is obtained when discarding data that are above the $K_{J\ limit}$. When data obtained by ORNL are analyzed in a similar way, the large CT samples lead to T_0=−65°C [19].

According to E1921, PCCv specimens result in T_0=−77°C ((−68.6−84.7)/2). Figure 11 shows that many CT specimens lie outside the 5% bound. However, Figure 12 shows that the 1% bounds fit the experimental data very well. The K_{IC} ASME curve based on RT_{To} underestimates the lower bound, while an extra margin remains if RT_{NDT} is used. It is important to emphasize here that T_0 is based on PCCv samples. When T_0 is taken equal to −63°C, a much better agreement to the experimental data is found.

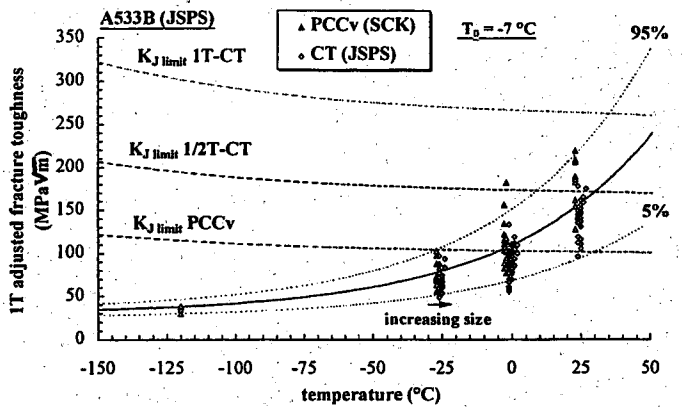

Figure 8. Master curve and associated confidence bounds for A533B (JSPS) material. JSPS round robin data are also included for comparison.

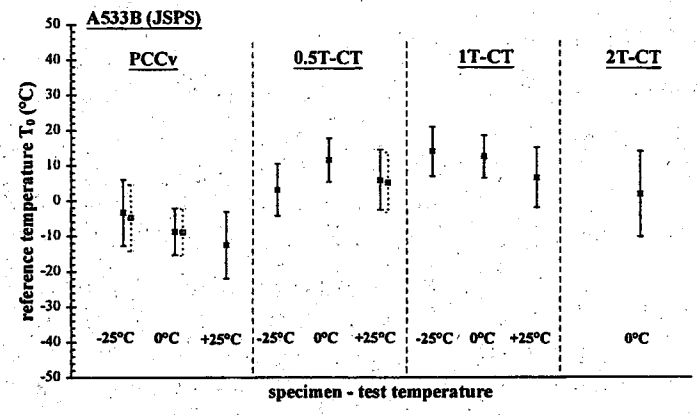

Figure 9. Effect of test temperature and specimen geometry and size on the reference temperature, T_0. Charpy size specimens result in reference temperature of 15°C lower than the CT samples.

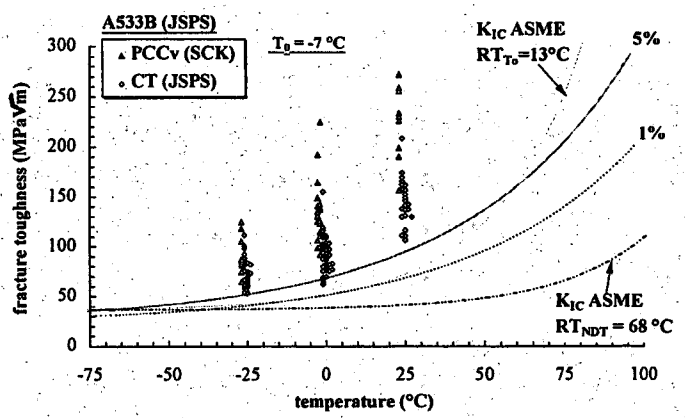

Figure 10. Comparison of 73W fracture toughness data to lower bound curves: ASME K_{IC} versus probability curves.

Table 11. Master curve transition parameters for A533B (JSPS).

specimen	N	T	T_0	K_0	m	method	Remark
PCCv	6	−120	20.9	36.2	5.2	1	no size correction, all valid
	10	−25	−3.4	81.8	4.0	1	all
	10	−25	−3.1	81.6	4.0	3	censor N=r=10
	10	−25	−4.8	83.3	4.0	2	censor E1921 N=10, r=9
	9	−25	1.6	77.3	4.4	4	censor N=r=9
	20	0	−8.8	121.6	3.6	1	all
	20	0	7.2	97.8	17.3	3	censor N=r=20
	20	0	−9.0	121.9	17.3	2	censor E1921: N=20, r=7
	7	0	13.2	90.6	9.5	4	censor N=r=7
	10	25	−12.6	187.6	7.1	1	all (all not valid)
0.5T	16	−25	3.1	76.0	4.2	1	valid per E1921
	23	0	11.5	92.6	3.9	1	valid per E1921
	12	25	5.9	141.3	6.3	1	all
	11	25	8.7	135.5	10.6	4	only valid
	12	25	5.1	142.8	7.1	2	censoring per E1921
	12	25	6.4	140.1	7.1	3	
1T	18	−25	14.0	67.6	6.1	1	valid per E1921
	24	0	12.5	91.4	6.9	1	valid per E1921
	12	25	6.5	140.0	7.4	1	valid per E1921
2T	6	0	1.8	105.2	7.8	1	valid per E1921

Table 12. Master curve analysis of 73W weld material. All PCCv specimens are 20% side grooved.

specimen	N	T	r	T_0	K_0	m	method	remark
PCCv	8	−100	--	−68.6	73.2	6.6	1	valid per E1921
	11	−80	--	−89.0	122.0	2.8	1	all data
	7	−80	7	−66.1	89.9	4.2	4	only valid data
	11	−80	10	−77.7	104.4	4.2	3	censoring N=r=11
	11	−80	7	−84.7	114.9	4.2	2	censoring E1921
CT	--	--	--	−65(1)			1	CT (ORNL data [6])

Notes: (1) T_0 is determined using the Wallin's multiple temperature method. Note that plane strain elastic modulus is used for J - K_J conversion. (T_0=−61°C when plane stress elastic modulus is used).

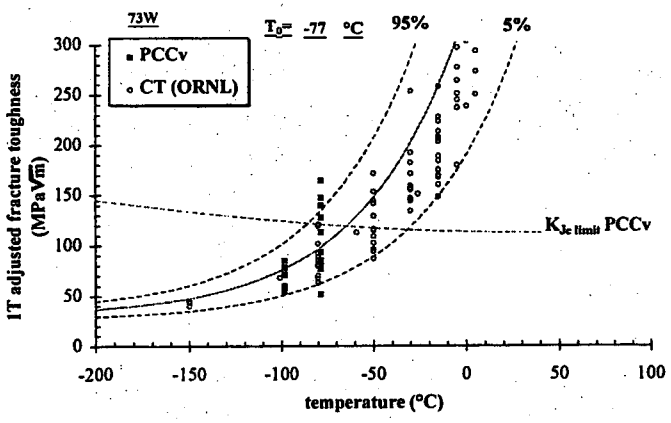

Figure 11. Master curve and associated confidence bounds for the 73W weld material. ORNL data are also included for comparison.

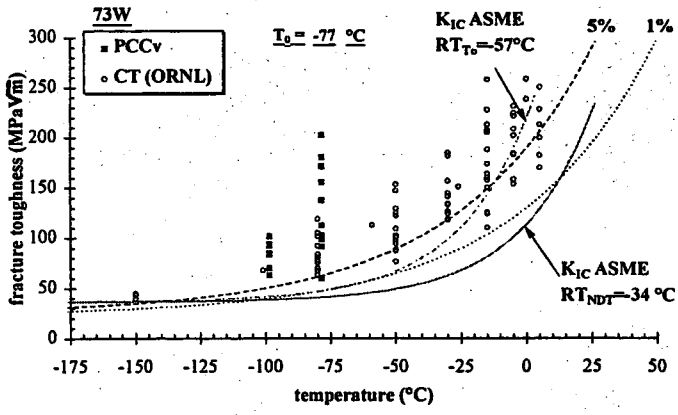

Figure 12. Comparison of 73W fracture toughness data to lower bound curves: ASME K_{IC} versus probability curve.

DISCUSSION

The E1921 standard is found to be a very efficient tool for characterizing fracture toughness in the transition regime. However, with increasing the fracture toughness databank, some minor modifications of the actual procedure will certainly improve the accuracy on T_0 determination. The use of the precracked Charpy geometry is found very promising although T_0 tends to be slightly lower than with large CT specimens.

Given the limited number of specimens, it is extremely difficult to separate the effects of size, geometry and test temperature from material variability. It should be understood here that there is a inherent material variability, but this inhomogeneity can be enhanced when comparing data of specimens taken from different locations.

Within all these uncertainties, it is found that test temperature does not significantly affect the determination of T_0, even when data are not fully satisfying the E1921 requirements. In comparison to large samples, the PCCv samples lead to T_0 values which are 5 to 20°C lower (see Table 13). The ASTM E1921 procedure is used for determining T_0. As a consequence, the censoring procedure as required by the above standard is used. This censoring procedure does not affect the final results: T_0 remains almost unchanged by application of the censoring procedure. Monte Carlo simulation performed by Scibetta [20] clearly indicates the non conservative character of this censoring procedure. A better agreement is found if only valid data are taken into account or if non valid data are replaced by the $K_{J\,limit}$ and N=r.

The E1921 discards specimens that do not fulfill the crack front uniformity (individual crack lengths within ±7% of the average crack length, or within 0.5 mm, whichever is larger). On this basis 90% of the data for 22NiMoCr37, which were plain sided, should not be used for T_0 determination. It is shown that despite the non uniformity of the crack, T_0 agrees very well with the one determined with the large samples. It would be advisable to take into account such data and only mention the crack front non-uniformity in the test report.

A question arises regarding the appropriateness of the M=30 limit factor in E1921: is it too low? Nevalainen and Dodds [11] performed detailed 3D finite element calculations. These calculations suggest M=60 for the material under consideration. Table 13 shows that the agreement is much improved in comparison to CT geometry if M=60 is used instead of M=30. Another very interesting geometry, the circumferentially-cracked round bar (CRB), leads to very similar results (see Table 13). Scibetta [20-21] has shown that loss of constraint appears very early in this geometry. By scaling this geometry to the small scale yielding condition, the results shown in Table 13 are in good agreement with large samples. The size adjustment is applied to the volume rather than to the thickness in order to take loss of constraint into account, the small scale yielding (SSY) condition being the reference state.

In order to estimate the reliability the various lower bound curves, the temperatures corresponding to K=100 MPa√m are compared in Table 14. The K_{IC} ASME curve indexed by the RT_{NDT} is clearly shifted to higher temperature in comparison to a RT_{To}-indexed K_{IC} curve, and to a 1% curve. A very good agreement is noticed between these last curves, the 1% curve being more conservative. This is illustrated in Figure 13 where all PCCv data are plotted as a function of $(T-T_0)$ and compared to RT_{To} and 1% curves. In the region of test temperature. In the temperature range of T_0±30°C, both curves are identical. For higher test temperatures, the two curves largely deviate from each other. In particular, above T_0+30°C, more experimental data are required to estimate the reliability of both curves. The current regulation based on RT_{NDT} gives an additional 20 to 40°C extra margin to the actual lower bound.

Table 13. Influence of the $K_{J\,limit}$. A better agreement is obtained when increasing M to 60.

M		22NiMoCr37	JRQ	A533B (JSPS)	73W
30	T_0 PCCv	−100	−54	−7	−77
30	T_0 large samples	−101	−43	8	−64
60	T_0 PCCv	−95	−42[1]	5	−69
60	T_0 large samples	−101	−43	8	−64
SSY	T_0 CRB samples	−90	−36	14	--

Notes: (1) Due to the limited number of samples, T_0 is determined using the E1921 censoring procedure (N=6, r=4).

Table 14. Comparison between various lower bound curves expressed at the 100MPa√m K_{Jc} level.

$T_{100MPa\sqrt{m}}$	22NiMoCr37	JRQ	A533B (JSPS)	73W
5% curve	−64	−18	29	−41
RT_{To} curve	−57	−6	41	−29
1% curve	−45	6	53	−17
K_{IC} ASME curve	−12	13	96	−6

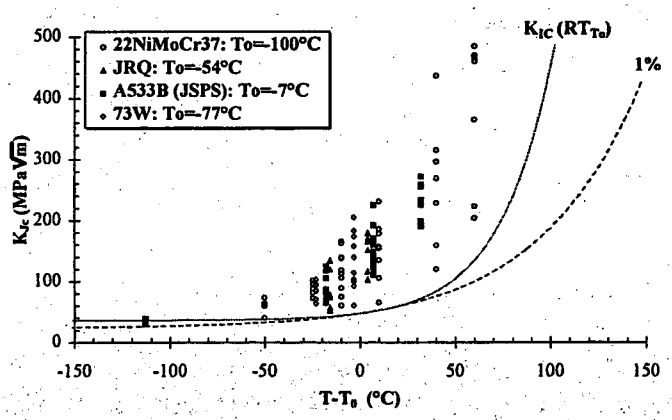

Figure 13. Comparison of PCCv fracture toughness data to T_0-based predictive lower bound curves for the four materials. Very good agreement between experimental and predictive curves is observed. At the upper transition region, the 1%-curve is more conservative than the RT_{To}-based curve.

CONCLUSIONS

This work has shown that the Charpy size specimen combined with the Master Curve approach can reliably characterize fracture toughness in the transition regime. The determination of the reference temperature, T_0, according to ASTM E1921 standard by using a limited number of samples, is found independent from test

temperature. However, it is important to associate with T_0 a confidence interval that depends on the size of the data set.

With small specimens, the application of the censoring procedure becomes sometimes necessary, in particular when testing at temperatures close to or higher than T_0. It is observed that the censoring procedure as recommended by the ASTM E1921 standard does not affect the results, which can lead sometimes to non conservative results. The T_0 derived from PCCv specimens lie 5 to 20°C below those derived from large samples (mainly CT). Increasing the M factor of the $K_{J\ limit}$ to 60, as suggested by finite element calculations, largely improves the agreement. However, considering the limited experimental effort presented here, further work is needed to confirm this finding.

For safety assessment considerations, the lower bound fracture toughness is of prime importance. It is found that the 1% curve and the RT_{T_0} based ASME curve are very good estimates of the fracture toughness lower bound. Above T_0+30°C, more experimental data are required to estimate the reliability of both curves. Comparison to the ASME K_{IC} curve (indexed to RT_{NDT}) indicates that the latter results in an over conservative temperature margin of about 30°C.

ACKNOWLEDGMENTS

The authors are grateful to R.K Nanstad from ORNL for providing the 73W weld material, and to K. Onizawa from JAERI who made all the necessary arrangements with the Japan Steel Works Ltd. to provide the A533B (JSPS) steel. The authors acknowledge the technical support of the LHMA team, in particular L. Van Houdt and A. Pellettieri who performed most of the tests reported here, and R. Mertens for specimen fabrication.

REFERENCES

[1] Wallin K., "Statistical modelling of fracture in the ductile-to-brittle transition region", Defect Assessment in Components - Fundamentals and Applications, ESIS/EGF9, Edited by J.G. Blauel and K.-H. Schwalbe, 1991, Mechanical Engineering Publications, London, pp. 415-445.

[2] ASTM E1921, Test method for the determination of reference temperature, T_0, for ferritic steels in the transition regime, Annual Book of ASTM Standards, Section 3, Vol. 03.01, 1998.

[3] Chaouadi, R., Analysis of fracture toughness behaviour of 22NiMoCr37 steel in the transition regime (SM&T Round Robin), SCK•CEN Report BLG-799, December, 1998.

[4] "Standard Test Method for Fracture Toughness within Ductile-Brittle Transition Range," Standard of the 129th Committee, Japan Society for the Promotion of Science, 1995, (in Japanese).

[5] van Walle E., Chaouadi R., Scibetta M, Puzzolante J.L., Fabry A. and Van de Velde J., Belgian contribution to the IAEA CRP-IV programme on "Assuring Structural Integrity of Reactor Pressure Vessel Steels", SCK•CEN Report BLG-754, October, 1997.

[6] Nanstad R.K., Haggag F.M., McCabe D.E., Iskander S.K., Bowman K.O. and Menke B.H., "Irradiation effects on fracture toughness of two high-copper submerged-arc welds, HSSI series 5", NUREG/CR-5913, ORNL/TM-12156/V1, 1992.

[7] ESIS P2-92, Procedure for determining the fracture toughness behaviour of materials, European Structural Integrity Society, January 1992.

[8] Mudry M. and Di Fant M., A round robin on the measurement of local criteria, Final Report RE 93.319, 1993.

[9] Manufacturing history, initial mechanical properties and radiation damage in the IAEA reference steel JRQ of ASTM A533 type B Class 1 steel plate.

[10] Gérard R., Survey of national regulatory requirements, AMES Report n°4, June, 1995.

[11] Nevalainen M. and Dodds R.H. Jr., Numerical investigation of 3-D constraint effects on brittle fracture in SE(B) and C(T) specimens, UILU-ENG-95-2001, University of Illinois, February 1995.

[12] Koppenhoefer K.C and Dodds R.H. Jr., Loading rate effects on cleavage fracture of precracked CVN specimens: 3-D studies, Engineering Fracture Mechanics, Vol. 58, No. 3, 1997, pp. 249-270.

[13] Kirk M., Lott R., Server W., Hardies R. and Rosinski S., Bias and precision of T_0 values determined using ASTM standard E1921-98 for nuclear pressure vessel steels, Effect of Radiation on Materials,: 19th International Symposium, M.L Hamilton, M. Grossbeck and A.S. Kumar, Eds, American Society for Testing and Materials, 1998.

[14] Chaouadi R. and Scibetta M., On the use of the Master Curve concept and the Charpy size specimen to characterize fracture toughness in the transition regime: Part I: RPV steel with high upper Shelf - 22NiMoCr37 SCK•CEN report, R-3294, December 1998.

[15] Scibetta M, Chaouadi R. and van Walle E., Status report on the use of the CRB for the measurement of fracture toughness of RPV steels, SCK•CEN Report BLG-763, February, 1998.

[16] van Walle E., Fabry A., Puzzolante J.L., Pouleur Y., Verstrepen A., Wannijn J.P. and Van de Velde J., Belgian contribution to the IAEA Phase 3 Coordinated Research Programme on "Optimisation of Reactor Pressure Vessel Surveillance Programmes and Their Analysis", SCK•CEN Report, November, 1993.

[17] Chaouadi R. and Scibetta M., On the use of the master curve concept and the Charpy size specimen to characterize fracture toughness in the transition regime: Part II: RPV steel with low upper shelf - A533B (JSPS), SCK•CEN report, R-3326, March 1999.

[18] Chaouadi R., van Walle E., Fabry A., Scibetta M. and Van de Velde J., Fracture toughness of precracked Charpy specimens of irradiated 73W weld material, Effect of Radiation on Materials,: 19th International Symposium, M.L Hamilton, M. Grossbeck and A.S. Kumar, Eds, American Society for Testing and Materials, 1998.

[19] Chaouadi, R., Fracture toughness measurements in the transition regime using small size samples, Small Specimen Test Techniques, ASTM STP 1329, W.R. Corwin, S.T. Rosinski and E. van Walle, Eds., American Society for Testing and Materials, 1998, pp. 214-237.

[20] Scibetta M., Contribution to the evaluation of the circumferentially-cracked round bar for fracture toughness determination of reactor pressure vessel steels, Ph.D. thesis, May, 1999.

[21] Scibetta M, Chaouadi R. and van Walle E., Fracture toughness evaluation of circumferentially-cracked round bars: theoretical aspects, submitted for publication, 1998.

PVP-Vol. 393

FRACTURE, FATIGUE, AND WELD RESIDUAL STRESS

presented at

THE 1999 ASME PRESSURE VESSELS AND PIPING CONFERENCE
BOSTON, MASSACHUSETTS
AUGUST 1–5, 1999

sponsored by

THE PRESSURE VESSELS AND PIPING DIVISION, ASME

principal editor

J. PAN
UNIVERSITY OF MICHIGAN

contributing editors

M. T. KIRK
WESTINGHOUSE ELECTRIC COMPANY

G. M. WILKOWSKI
ENGINEERING MECHANICS CORP.

K. K. YOON
FRAMATOME TECHNOLOGIES

P. DONG
BATTELLE

Y. J. CHAO
UNIVERSITY OF SOUTH CAROLINA

THE AMERICAN SOCIETY OF MECHANICAL ENGINEERS
Three Park Avenue / New York, N.Y. 10016